Synthetic Metals 160 (2010) 238–243

Contents lists available at ScienceDirect

Synthetic Metals

journal homepage: www.elsevier.com/locate/synmet

A photoemission study of interfaces between organic semiconductors and Co as well as Al_2O_3/Co contacts

M. Grobosch[a,*], C. Schmidt[a], W.J.M. Naber[b], W.G. van der Wiel[b], M. Knupfer[a]

[a] IFW Dresden, Helmholtzstrasse 20, 01069 Dresden, Germany
[b] NanoElectronics Group, MESA+ Institute for Nanotechnology, University of Twente, PO Box 217, 7500 AE Enschede, The Netherlands

ARTICLE INFO

Article history:
Received 14 March 2009
Received in revised form 5 July 2009
Accepted 8 September 2009
Available online 24 October 2009

Keywords:
Spintronics
Photoemission spectroscopy
Energy-level alignment
Pentacene
Rubrene

ABSTRACT

We have studied the energy-level alignment of ex situ, acetone cleaned Co and Al_2O_3/Co contacts to the organic semiconductors pentacene and rubrene by combined X-ray and ultraviolet photoemission spectroscopy. Our results demonstrate that the work function under these conditions is smaller than in the in situ cleaned, atomically clean case. Moreover, the studied interfaces are characterized by very small, short range interfaces dipoles and substantial injection barriers for holes. This represents essential information in view of their use in organic spintronic devices. Our core-level photoemission spectroscopy measurements rule out chemical reactions.

1. Introduction

Organic spin electronics, also referred to as organic spintronics, has come into focus as a new and promising research field in recent years [1]. In this context, organic spintronics comprises the application of organic materials for the transport and the control of spin-polarized information. The demonstration of the giant magnetoresistance effect (GMR) in metallic heterojunctions [2,3], as well as tunneling magnetoresistance (TMR) [4] in ferromagnetic tunnel junctions are considered important breakthroughs in the field of spin electronics. It has also initiated further applications regarding magnetic memory devices in which the active control and the manipulation of spin degrees of freedom is anticipated [5]. For the injection/detection of spin-polarized electrons in an organic semiconductor, a ferromagnetic (FM) electrode with a substantial degree of electron spin-polarization in the conduction band is required. A lot of activity is presently going on to inject spin-polarized currents in organic semiconductors [6–12]. One of the earliest reports is by Dediu et al. [13], who reported the possibility of injecting spin-polarized currents in organic semiconductors and reported room temperature magnetoresistance for α-sexithiophene as the spin transport medium between two $La_{0.7}Sr_{0.3}MnO_3$ (LSMO) electrodes. A spin-valve effect in a vertical geometry device using tris(8-hydroxyquinolino)-aluminum (Alq_3) between a 60-monolayer thick $La_{0.7}Sr_{0.3}MnO_3$ film as bottom electrode and a top electrode of 3.6 nm Co was reported in 2004 by Xiong et al. [8]. Furthermore, Santos et al. [11] reported a tunneling of the spin across a thin layer of Alq_3 up to room temperature. All these observations can be regarded as encouraging for the field of organic spintronics in which the flexibility and variability of the organic semiconducting material is combined with a further degree of freedom for switching or controlling a device via external magnetic or electric fields. Organic materials are mainly consisting of light elements, which leads to weak spin–orbit coupling. Despite the presence of nuclear spins, the hyperfine interaction in organic materials is possibly also weak [1]. Therefore, organic semiconductors are believed to have a long spin relaxation time and consequently a large spin diffusion length λ_S. In 2008 Shim et al. [14] reported a large spin diffusion length of 13.3 nm in amorphous rubrene, showing the great potential of organic semiconductors for organic spintronic development.

Rubrene ($C_{42}H_{48}$) as well as pentacene ($C_{22}H_{14}$) are characterized by high charge carrier mobilities, for organic standards. For rubrene high hole mobilities in the range of 15–20 cm^2/Vs were reported for high-purity single-crystals [15,16]. Also pentacene exhibits high charge carrier mobilities from typical 0.4–1 cm^2/Vs for thin-film transistors (TFTs) made from good quality pentacene films [17] to 35 cm^2/Vs for high-purity single-crystals [18]. Consequently, rubrene and pentacene are promising candidates for future electronic devices as well as for the investigation of spin transport properties. The choice of Co as electrode material comes from the fact that Co is a commonly used ferromagnetic material

* Corresponding author.
E-mail address: M.Grobosch@ifw-dresden.de (M. Grobosch).

0379-6779/$ – see front matter © 2009 Elsevier B.V. All rights reserved.
doi:10.1016/j.synthmet.2009.09.014

for the injection as well as detection of spin-polarized electrons in spintronic devices [8,11,19] with a bulk spin-polarization of around 45% [1,20,21]. A common problem for spin injection and detection using a ferromagnetic metal (such as Co) electrode is the so-called conductivity mismatch [1,22,23]. To solve the conductivity mismatch problem two solutions are possible: (i) a fully spin-polarized FM material, e.g. a half-metal such as LSMO which is an attractive rare-earth compound characterized by nearly 100% spin-polarization of charge carriers [24] is used as the electrode material. Recently, LSMO electrodes have been applied in spintronic devices with organic semiconductor thin films [8,13,19]. (ii) The introduction of a thin tunnel barrier (e.g. Al_2O_3) as a large spin-dependent resistance in between the ferromagnetic electrode and the organic semiconductor is another possible solution for the conductivity mismatch problem [1,23]. The fabrication of a tunnel barrier, Al_2O_3 in our case, is important to overcome the conductivity mismatch between the metal electrodes and a semiconductor spacer, which is a problem in semiconductor spintronic devices [22,23]. The insertion of a thin tunnel barrier of Al_2O_3 has been successfully applied in spintronic devices [11,19].

Up to now only a few studies on interfacial properties of spintronic relevant contact materials (e.g. LSMO, Co) and organic semiconductors using photoemission spectroscopy were published. Zhan et al. have published in 2007 and 2008 interface studies for the organic semiconductor Alq_3 in contact to the electrode materials LSMO [25] and Co [26]. The interfacial properties between the two organic semiconductors α-sexithiophene (α-6T) and copper-phthalocyanine (CuPc) were published in 2008 and 2009 by our group reflecting the influence of the applied in situ cleaning [27] as well as ex situ cleaning [28] procedure to the used LSMO thin film contacts. The interface properties of the organic semiconductor pentacene in contact with Co were previously published by Tiba et al. [29] and Popinciuc et al. [30]. The influence of a thin tunnel barrier on the interfacial structure of interfaces between Co and pentacene was studied in 2007 by Popinciuc et al. [31]. In the past, the interfaces between various metallic electrodes and organic semiconductors have been studied widely [32–37]. Most of these interfaces are characterized by the presence of an interface dipole confined to a thin interfacial layer, whereas the origin of this interface dipole is not fully understood yet [38,39].

In this contribution, we present a detailed analysis of interfaces for the two archetype organic semiconductors, pentacene and rubrene, in contact with ex situ cleaned Co as well as Al_2O_3/Co thin films. We have studied the energy-level alignment of ex situ, acetone cleaned Co and Al_2O_3 contacts to the organic semiconductors pentacene and rubrene using combined X-ray and ultraviolet photoelectron spectroscopy. Our results demonstrate that the work function under these conditions is smaller than in the in situ cleaned, atomically clean case. Moreover, all studied interfaces are characterized by very small, short range interface dipoles and substantial injection barriers for holes. Our core-level photoemission spectroscopy measurements rule out chemical reactions for all three interfaces. This represents essential information in view of their use in organic spintronic devices.

2. Experimental details

The presented combined X-ray and ultraviolet photoemission spectroscopy studies were performed using a commercial PHI 5600 spectrometer, which is equipped with two photon sources. Monochromatized photons with an energy of 1486.6 eV from an Al Kα source for X-ray photoemission spectroscopy (XPS) and photons from a He-discharge lamp with an energy of 21.21 eV for ultraviolet photoemission spectroscopy (UPS) are provided. All ultraviolet photoemission spectroscopy measurements were done by applying a bias voltage of −9 V to distinguish between the analyzer and sample cutoffs and the spectra were additionally corrected for the contributions of He-satellite radiation. The total energy resolution of the spectrometer was determined by analyzing the width of an Au Fermi edge to be about 350 meV (XPS) and 100 meV (UPS), respectively.

As substrates for our organic layer, we used ex situ cleaned polycrystalline Co (40 nm) and Al_2O_3 (3 nm)/Co (40 nm) films. For the Co as well as the Al_2O_3/Co films a SiO_2 (300 nm) coated silicon wafer was used as substrate. The substrates were cleaned in a cleanroom environment with acetone, IPA, and DI-water. In an UHV chamber (base pressure 1×10^{-10} Torr) Co as well as Al were deposited via e-beam evaporation. First the Co was deposited with an evaporation rate of 0.1 nm/s. For the Al_2O_3/Co substrates Al was evaporated in a second step also with a rate of 0.1 nm/s. The Al coated samples were transferred to a load lock for the plasma oxidation without breaking the vacuum. The plasma oxidation was performed with a pressure of 100 mTorr and a voltage of 800 V, giving a current of 85 mA. The Al/Co samples with a thickness of the Al layer of max. 2.5 nm were oxidized for 30 min resulting in a 3 nm thick Al_2O_3 layer thickness. We determine the height of the Al film before the oxidation with a crystal inside the evaporator. The thickness of the Al_2O_3 layer will be about 20% larger than that of the Al film. The Co and Al_2O_3/Co substrates were exposed to ambient conditions and subsequently cleaned ex situ using acetone (2 min bath in acetone and additionally rinsing the sample for 1 min). We point out that in the fabrication of organic electronic devices, e.g. devices which used $La_{0.7}Sr_{0.3}MnO_3$ as the bottom-electrode material, such a treatment is also applied [7–10]. By applying this kind of ex situ cleaning it is possible to probe bottom contacts as they are applied. In this way we are able to provide an energy-level alignment that is of relevance for the understanding and modeling of corresponding devices. From our core-level photoemission studies we can conclude that the Co as well as Al_2O_3/Co surfaces are still covered with a contamination layer consisting of carbon and oxygen. The composition of this contamination layer was determined to be on average 70% carbon and 30% oxygen. The thickness of the contamination layer is about 1–2 nm. The thickness of the contamination layer was estimated from photoemission intensities. In previous publications it was already demonstrated that ex situ cleaning results in such a contamination layer independent on the individual details of the applied treatment [28,40,41].

Thin films of rubrene and pentacene were deposited by in situ thermal evaporation on Co and Al_2O_3/Co thin films with a typical evaporation rate of 0.1–0.25 nm/min in a preparation chamber (base pressure 2×10^{-10} mbar), which is directly connected to the analyzer chamber. Subsequently, the films were transferred to the analyzer chamber without breaking the vacuum and characterized taking a full-range XPS spectrum. The number of impurities in the films was very small and below the detection limit of the XPS due to the ultrahigh vacuum conditions during the preparation process of the organic films. To estimate the thickness of the individual organic overlayers we have monitored the attenuation of the intensity of the Co2*p* substrate peak for the Co thin films as well as the O1*s* substrate peak for the Al_2O_3/Co films [42,43] due to the organic film. Considering the procedure of Seah and Dench [43] we have calculated the mean free path of the electrons in rubrene to be about 2.27 and 2.11 nm in pentacene films, for the kinetic energy of 955.6 eV for the O1*s* signal from the contaminated substrates and a density of 1.27 g/cm^3 for rubrene and 1.32 g/cm^3 for pentacene [44,45]. We point out that this procedure to determine the thickness of the organic layer is only correct for layer-by-layer growth. If the organic film does not grow uniformly, this method underestimates the film thickness.

3. Results and discussion

3.1. Electrode surface characterization

We have mentioned above that the contamination layer on top of the Co and Al_2O_3/Co films consists of carbon and oxygen. To show this in more detailed way we present in Fig. 1 the Co2$p_{3/2}$ core-level emission feature for a contaminated Co surface after applying an ex situ cleaning treatment as described above. The Co2*p* emission shows clearly a three-peak structure (peaks labelled with I, II, and III). The first peak (I) appears at 778.2 eV for the Co2$p_{3/2}$ component. This binding energy is approximately equal to the binding energy of metallic Co (778.3 eV [46] for Co2*p*). The two peaks at higher binding energies of 780.8 eV (Peak II) as well as 786.0 eV (Peak III) match very well the peak structure in the spectrum of native cobalt oxide [26,31,47]. From our core-level spectroscopy measurements of the Co2*p* emission we can conclude that the contaminations on top of ex situ cleaned Co surfaces results in a native cobalt oxide layer. Our separate measurements of the C1*s* and O1*s* core-level (spectra not shown) of ex situ cleaned Co surfaces agree with this result.

We have also applied the above described ex situ cleaning procedure to the Al_2O_3/Co substrates. In Fig. 2 the results of the core-level spectroscopy measurements are depicted for the Co2$p_{3/2}$ (panel a) peak as well as the Al2*p* (panel b) core-level emission from an ex situ cleaned Al_2O_3/Co substrate. The Co2*p* core-level emission consists of one single peak at a binding energy of 778.3 eV (equal to the binding energy of pure (metallic) Co of 778.3 eV [46,47]) with a small contribution of native Co oxide (Peak II at 779.4 eV) [26,31,47]. As expected from previous publications the Al_2O_3 layer on top of Co prevents the oxidation of the Co film. The spectra of the Al2*p* emission feature from the substrate shows a two-peak structure indicating the presence of reduced species at the lower binding energy side (Peak I at 72.7 eV). The structure at higher binding energies (Peak II) at 75.6 eV is in good agreement to the energy of the Al2*p* emission in Al_2O_3.

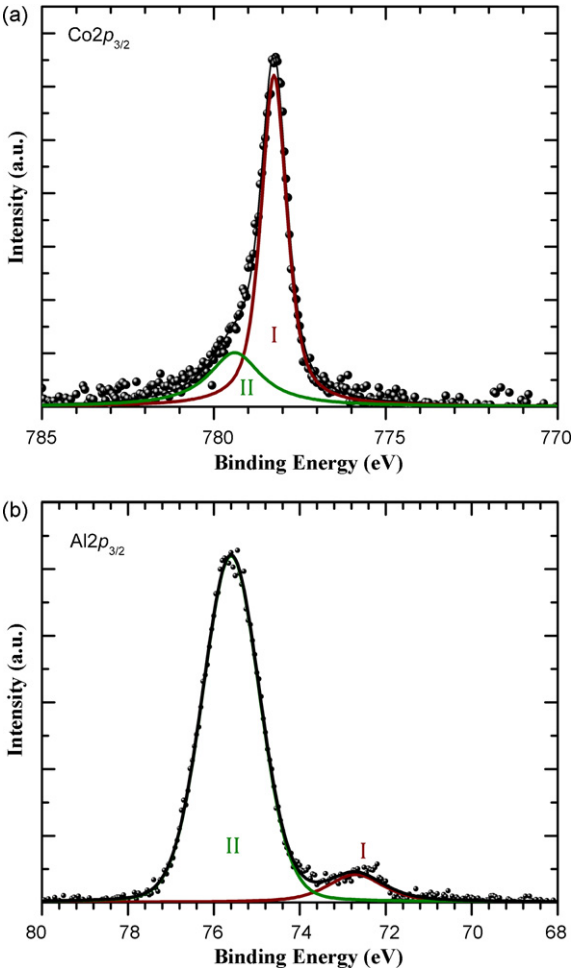

Fig. 2. Co2*p* and Al2*p* core-level photoemission spectra of an ex situ cleaned Al_2O_3/Co surface for a thickness of the Al_2O_3 layer of 3 nm.

3.2. Electronic properties of the interfaces

From the obtained core-level photoemission spectroscopy studies we can obtain some first information about the interfacial electronic properties. In Fig. 3 we summarize the data for the Co2*p* (panel a) and Al2*p* (panel b) core-level emission features for the pentacene/Co as well as pentacene/Al_2O_3/Co interface depending on the film thickness of pentacene. The spectral shape of the Co2*p* and Al2*p* core-level remain unchanged independent of the respective film thickness. Also the binding energy of the core-level is constant. Also in the core-level photoemission spectra of the Co2*p* and Al2*p* (not shown) emissions for the rubrene/Al_2O_3/Co interface we observed constant binding energies as well as an unchanged spectral shape with an increase in the rubrene film thickness. This evidences that the contamination layer is closed and prevents chemical reactions between the substrates and the organic semiconductors.

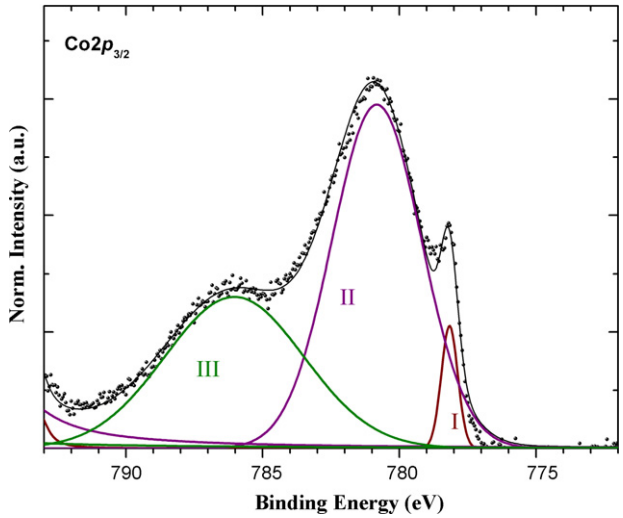

Fig. 1. Co2*p* core-level photoemission spectra of a contaminated Co surface.

In Fig. 4 the valence-band photoemission data of the pentacene/Al_2O_3/Co (panel a) as well as rubrene/Al_2O_3/Co (panel b) interface as a function of the organic semiconductor film thickness are depicted. These data provide us with a detailed knowledge of the interface properties of these two interfaces. In the top spectra of each panel the valence-band from the ex situ cleaned Co as well as Al_2O_3/Co surfaces are shown. In both cases the characteristic valence-band features of the substrate are suppressed due to the presence of the contamination layer on top of the substrate surface. Consequently, the valence-band region is featureless as expected for such contaminated contacts. The work function of the ex situ cleaned Co surface used in our studies was measured to be 4.3 eV within an experimental error of 0.1 eV. This value is substantially smaller than that of a clean polycrystalline Co surface (5.0–5.1 eV) [26,29,30,48]. The reduced work function due to presence of the contamination layer presents an expected result which is in good agreement to previously pub-

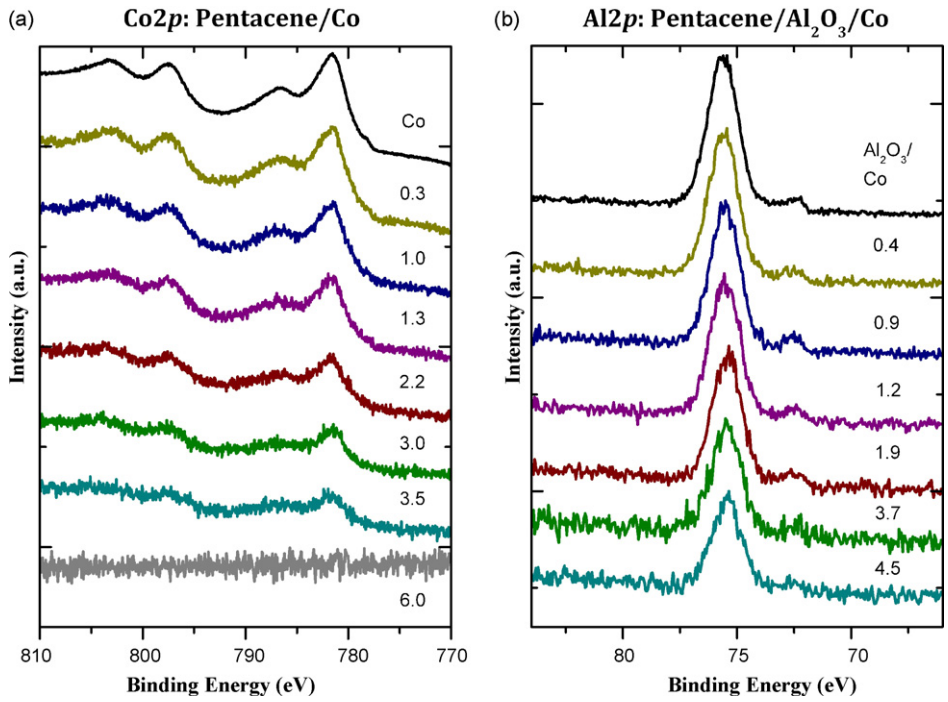

Fig. 3. Co2*p* (left panel) and Al2*p* (right panel) core-level photoemission spectra for an increasing pentacene film thickness (all values for the pentacene film thickness are given in nm).

lished interface studies using ex situ cleaned electrode materials [28,40,41]. In the case of ex situ cleaned Al_2O_3 surfaces a work function ranging from 3.1 to 3.5 eV was measured. The typical valence-band features of the organic semiconductors pentacene and rubrene become more and more visible with an increase in the organic semiconductor film thickness. In the case of contaminated rubrene/Al_2O_3/Co and pentacene/Al_2O_3/Co interface (see e.g. Fig. 4) as well as for pentacene/Co interfaces (not shown) their energy position is almost independent of the corresponding pentacene film thickness. Consequently the energy-level alignment concerns only a thin interfacial region. The individual features of the pentacene valence-band are in good agreement with previous publications [49,50]. Parallel to the situation of the core-level emission features the energy position of the typical valence-band features of

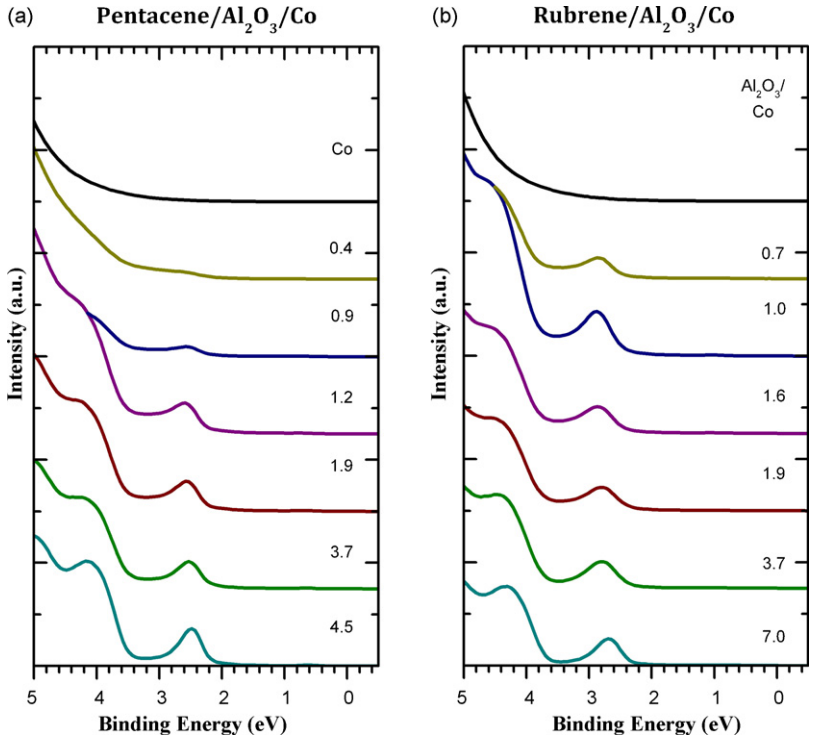

Fig. 4. Valence-band photoemission data for the pentacene/Al_2O_3/Co interface (left panel) and rubrene/Al_2O_3/Co interface (right panel) with increasing organic semiconductor film thickness (all values for the pentacene and rubrene film thickness are given in nm).

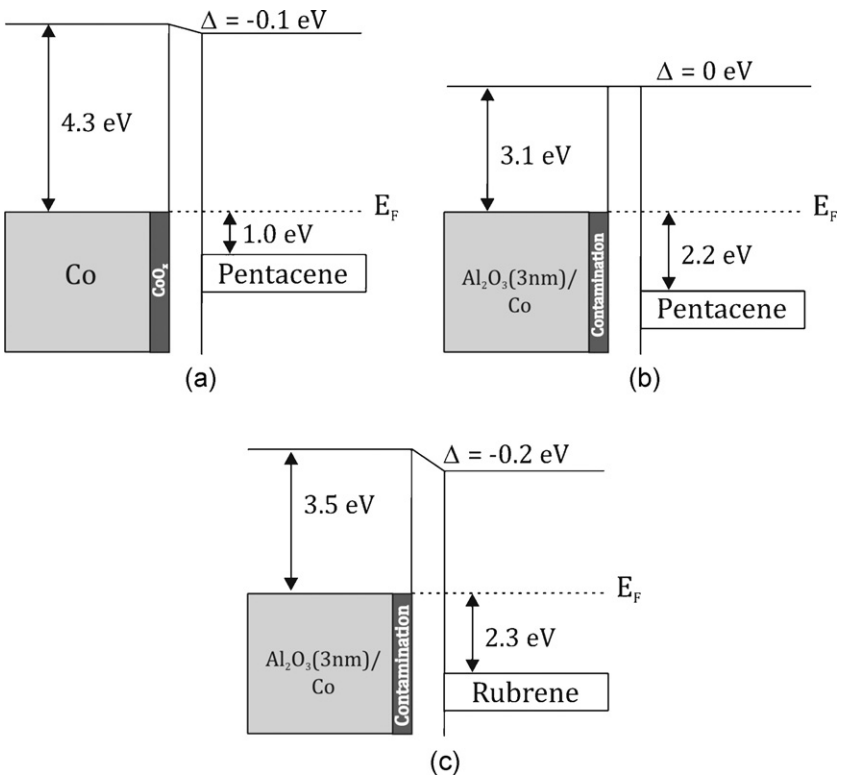

Fig. 5. Schematic energy-level diagrams of contaminated interfaces between Co and Al_2O_3/Co and the organic semiconductors pentacene and rubrene.

rubrene is also constant with increasing rubrene film thickness as depicted in Fig. 4b. Therefore, the energy-level alignment at the rubrene/Al_2O_3/Co interface also concerns to a thin interfacial layer. Previously reported valence-band studies [51,52] on rubrene interfaces shows a good agreement with the individual features of the observed rubrene valence-band. The point of interest here is the onset of the spectral feature at the lowest binding energy side arising from photoemission from the highest occupied molecular orbital (HOMO). This represents the barrier for hole injection (Φ_{bh}) at the respective interface. The low binding emission edge of the valence-band onset was determined by linear extrapolation. We estimate the uncertainty of this procedure to be 0.1 eV. The hole injection barrier at both interfaces is found to be 1.0 and 2.2 eV for the pentacene/Co and the pentacene/Al_2O_3/Co interfaces, respectively. For the rubrene/Al_2O_3/Co interface the barrier for hole injection was determined to be 2.3 eV.

3.3. Energy-level alignment

Our results of the energy-level alignment for the three studied interfaces are summarized in Fig. 5. The interface between pentacene and contaminated Co is characterized by a very small interface dipole of −0.1 eV (see Fig. 5a) confined to thin interfacial region. We attribute the strong change of the interface dipole compared to clean Co contacts to the reduced work function of Co due to the contamination layer on top if ex situ cleaned Co surfaces. The previously reported origin of the interface dipole at clean pentacene/Co interfaces in form of chemical reaction (hybridization) and formation of interface gap states [29,30] can be ruled out in case of contaminated pentacene/Co interfaces. Our UPS results show no evidence for the formation of interface gap states. Furthermore, the observed thickness independent and constant binding of the core-level emissions Co2*p* as well as of the HOMO exclude chemical reactions at the studied pentacene/Co interfaces. The in former studies [29,30] observed hybridization of the frontier orbital (HOMO) of pentacene and the Co3*d* bands is precluded owing to the fact that the contaminations of carbon and oxygen result in a native Co oxide layer on the ex situ cleaned Co surfaces. This conclusion is also manifested by a featureless valence-band of the contaminated Co substrates as discussed before. In addition we observe a hole injection barrier of 1.0 eV equal to the barrier for hole injection at clean pentacene/Co interfaces (e.g. 1.0 eV [29,30]). In comparison to the results of clean pentacene/Co interfaces we could prove a reduction of the interface dipole by 0.9 eV and a comparable reduction of the Co work function by 0.8 eV. Thus, we conclude that the energy-level alignment at contaminated pentacene/Co interfaces is only influenced by the reduction of the Co work function due to the observed contamination layer.

In Fig. 5b and c the data of the energy-level alignment for the pentacene/Al_2O_3/Co and the rubrene/Al_2O_3/Co interfaces are depicted. For the rubrene/Al_2O_3/Co interface a very small, short range interface dipole of −0.2 eV could be observed. In the case of the pentacene/Al_2O_3/Co vacuum-level alignment is present. As discussed above we could determine a constant binding energy of the Co2*p* and Al2*p* core-level emissions as well as of the frontier orbitals (HOMO) with increasing organic semiconductor film thickness. Furthermore no interface gap states could be observed. Consequently, we conclude that both interfaces to the 3 nm thick Al_2O_3 tunnel barrier are free from chemical reactions. For both interfaces we could demonstrate a very large hole injection barrier of 2.2 ± 0.1 eV. Popinciuc et al. [31] demonstrated in 2007 that the hole injection barrier depends on the inserted thin aluminium oxide tunnel barrier. They report a hole injection barrier of 0.85 eV for a Al_2O_3 thickness of 1 nm for clean pentacene/Al_2O_3/Co interfaces. They report further that for a thin Al_2O_3 barrier of 0.6 nm the hole injection barrier decreases by 0.35 eV compared to the clean Co contact [30]. This means an improvement in the efficiency of the barrier for hole injection. In contrast to the clean Co and Al_2O_3/Co cases we observe an increase of the hole injection barrier for the 3 nm thick Al_2O_3 tunnel barrier for ex situ

cleaned contacts. The observed very small interface dipoles correspond nearly to the Schottky-Mott-Limit. In consequence the energy-level alignment is not influenced by charge transfer through the tunnel barrier. From the very high hole injection barriers it is expected for spintronic devices that less charge carriers will be able to tunnel through the interface. In conclusion the contact resistance at contaminated pentacene/Al_2O_3/Co and rubrene/Al_2O_3/Co interfaces will increase. To stress the relevance of this work done on organic semiconductor/Al_2O_3/Co samples, spin-polarized at room temperature using Al_2O_3/Co contacts has been demonstrated by Santos et al. [11]. In this work the organic semiconductor Alq_3 has been used as spacer material. Also spin injection into graphene has been demonstrated using Al_2O_3/Co electrodes [53] as well as spin-injection into silicon by a ferromagnetic/Al_2O_3 contact [54].

4. Summary

In summary we determined the energy-level alignment of ex situ, acetone cleaned Co and Al_2O_3 contacts to the organic semiconductors pentacene and rubrene. Our results demonstrate that the work function under these conditions is smaller than in the in situ cleaned, atomically clean case. Moreover, the studied interfaces are characterized by very small, short range interfaces dipoles (within the experimental error of 0.1 eV) and substantial injection barriers for holes. This represents essential information in view of their use in organic spintronic devices. Our core-level photoemission spectroscopy measurements rule out chemical reactions.

Acknowledgments

We thank R. Hübel, R. Schönfelder, S. Leger, and J.G.M. Sanderink for technical assistance. The project was funded by the DFG, Project No. KN 393/5 and KN393/9. This work is part of WGvdW's VIDI research program "Organic materials for spintronic devices", financially supported by the Netherlands Organisation for Scientific Research (NWO) and the Technology Foundation STW.

References

[1] W.J.M. Naber, S. Faez, W.G.v.d. Wiel, J. Phys. D: Appl. Phys. 40 (2007) 205.
[2] M.N. Baibich, J.M. Broto, A. Fert, F.N. Van Dau, F. Petroff, P. Eitenne, G. Creuzet, A. Friederich, J. Chazelas, Phys. Rev. Lett. 61 (1988) 2472.
[3] J. Barnas, A. Fuss, R.E. Camley, P. Grünberg, W. Zinn, Phys. Rev. B 42 (1990) 8110.
[4] J.S. Moodera, L.R. Kinder, T.M. Wong, R. Meservey, Phys. Rev. Lett. 74 (1995) 3273.
[5] S.A. Wolf, D.D. Awschalom, R.A. Buhrman, J.M. Daughton, S. von Molnar, M.L. Roukes, A.Y. Chtchelkanova, D.M. Treger, Science 294 (2001) 1488.
[6] E. Shikoh, A. Fujiwara, Y. Ando, T. Miyazaki, Jpn. J. Appl. Phys. 45 (2006) 6897.
[7] S. Majumdar, R. Laiho, P. Laukkanen, I.J. Vayrynen, H.S. Majumdar, R. Osterbacka, Appl. Phys. Lett. 89 (2006) 122114.
[8] Z.H. Xiong, D. Wu, Z.V. Vardeny, J. Shi, Nature 427 (2004) 821.
[9] S. Majumdar, H.S. Majumdar, R. Laiho, R. Osterbacka, J. Alloys Compd. 423 (2006) 169.
[10] Z.Y. Pang, Y.X. Chen, T.T. Liu, Y.P. Zhang, S.J. Xie, S.S. Yan, S.H. Han, Chin. Phys. Lett. 23 (2006) 1566.
[11] T.S. Santos, J.S. Lee, P. Migdal, I.C. Lekshmi, B. Satpati, J.S. Moodera, Phys. Rev. Lett. 98 (2007) 016601.
[12] W. Xu, G.J. Szulczewski, P. LeClair, I. Navarrete, R. Schad, G. Miao, H. Guo, A. Gupta, Appl. Phys. Lett. 90 (2007) 072506–072513.
[13] V. Dediu, M. Murgia, F.C. Matacotta, C. Taliani, S. Barbanera, Solid State Commun. 122 (2002) 181.
[14] J.H. Shim, K.V. Raman, Y.J. Park, T.S. Santos, G.X. Miao, B. Satpati, J.S. Moodera, Phys. Rev. Lett. 100 (2008) 226603.
[15] V. Podzorov, E. Menard, A. Borissov, V. Kiryukhin, J.A. Rogers, M.E. Gershenson, Phys. Rev. Lett. 93 (2004) 086602.
[16] V.C. Sundar, J. Zaumseil, V.M.E. Podzorov, R.L. Willett, T. Someya, M.E. Gershenson, J.A. Rogers, Science 303 (2004) 1644.
[17] D. Knipp, R.A. Street, B. Krusor, R. Apte, J. Ho, J. Non-Cryst. Solids 299–302 (2002) 1042.
[18] O.D. Jurchescu, J. Baas, T.T.M. Palstra, Appl. Phys. Lett. 84 (2004) 3061.
[19] V. Dediu, L.E. Hueso, I. Bergenti, A. Riminucci, F. Borgatti, P. Graziosi, C. Newby, F. Casoli, M.P.D. Jong, C. Taliani, Y. Zhan, Phys. Rev. B 78 (2008) 115203.
[20] O. Andreyev, Y.M. Koroteev, M.S. Albaneda, M. Cinchetti, G. Bihlmayer, E.V. Chulkov, J. Lange, F. Steeb, M. Bauer, P.M. Echenique, S. Blügel, M. Aeschlimann, Phys. Rev. B 74 (2006) 195416.
[21] M. Cinchetti, K. Heimer, J.-P. Wüstenberg, O. Andreyev, M. Bauer, S. Laxh, C. Ziegler, Y. Gao, M. Aeschlimann, Nat. Mater. 8 (2009) 115.
[22] G. Schmidt, D. Ferrand, L.W. Molenkamp, A.T. Filip, B.J. van Wees, Phys. Rev. B 62 (2000) 4790.
[23] A. Fert, H. Jaffrès, Phys. Rev. B 64 (2001) 184420.
[24] J.H. Park, E. Vescovo, H.J. Kim, C. Kwon, R. Ramesh, T. Venkatesan, Nature 392 (1998) 794.
[25] Y.Q. Zhan, I. Bergenti, L.E. Hueso, V. Dediu, M.P. de Jong, Z.S. Li, Phys. Rev. B 76 (2007) 045406.
[26] Y.Q. Zhan, M.P. de Jong, F.H. Li, V. Dediu, M. Fahlman, W.R. Salaneck, Phys. Rev. B 78 (2008) 045208.
[27] M. Grobosch, K. Dörr, R.G. Gangineni, M. Knupfer, Appl. Phys. A 95 (2009) 95.
[28] M. Grobosch, K. Dörr, R.B. Gangineni, M. Knupfer, Appl. Phys. Lett. 92 (2008) 023302.
[29] M.V. Tiba, W.J.M. de Jonge, B. Koopmans, H.T. Jonkman, J. Appl. Phys. 100 (2006) 093707.
[30] M. Popinciuc, H.T. Jonkman, B.J. van Wees, J. Appl. Phys. 100 (2006) 093714.
[31] M. Popinciuc, H.T. Jonkman, B.J. van Wees, J. Appl. Phys. 101 (2007) 093701.
[32] H. Ishii, K. Sugiyama, E. Ito, K. Seki, Adv. Mater. 11 (1999) 605.
[33] W.R. Salaneck, K. Seki, A. Kahn, J.J. Pireaux, Conjugated Polymer and Molecular Interfaces: Science and Technology for Photonic and Optoelectronic Applications, Marcel-Dekker, New York, 2002, and references therein.
[34] A. Kahn, N. Koch, W. Gao, J. Polym. Sci. B 41 (2003) 2529.
[35] M. Knupfer, H. Peisert, Phys. Stat. Sol. A 201 (2004) 1055.
[36] N. Koch, ChemPhysChem 8 (2007) 1438.
[37] N. Koch, J. Phys.: Cond. Matter 20 (2008) 184008.
[38] M. Knupfer, G. Paasch, J. Vac. Sci. Technol. A 23 (2005) 1072.
[39] H. Vazquez, W. Gao, F. Flores, A. Kahn, Phys. Rev. B 71 (2005), 041306(R).
[40] A. Wan, J. Hwang, F. Amy, A. Kahn, Org. Electron. 6 (2005) 47.
[41] M. Grobosch, M. Knupfer, Adv. Mater. 19 (2007) 754.
[42] H. Peisert, T. Schwieger, M. Knupfer, M.S. Golden, J. Fink, J. Appl. Phys. 88 (2000) 1535.
[43] M.P. Seah, W.A. Dench, Surf. Interface Anal. 1 (1979) 2.
[44] R.B. Campbell, J.M. Robertson, Acta Cryst. 15 (1962) 289.
[45] E.A. Silinsh, V. Capek, Organic Molecular Crystals: Interaction, Localization and Transport Phenomena, AIP Press, New York, 1994.
[46] J.F. Moulder, W.F. Stickle, P.E. Sobol, K.D. Bomben, Handbook of X-ray Photoelectron Spectroscopy, Perkin-Elmer Cooperation, 1992.
[47] B.V. Christ, Handbook of monochromatic XPS spectra: The Elements of Native Oxides, Wiley-VCH, Chichester, 2000.
[48] H.B. Michaelson, J. Appl. Phys. 48 (1977) 4729.
[49] N. Koch, I. Salzmann, R.L. Johnson, J. Pflaum, R. Friedlein, J.P. Rabe, Org. Electron. 7 (2006) 537.
[50] A. Vollmer, H. Weiss, S. Rentenberger, I. Salzmann, J.P. Rabe, N. Koch, Surf. Sci. 600 (2006) 4004.
[51] Y. Harada, T. Takahashi, S. Fujisawa, T. Kajiwara, Chem. Phys. Lett. 62 (1979) 283.
[52] L. Wang, S. Chen, L. Liu, D. Qi, X. Gao, A.T.S. Wee, Appl. Phys. Lett. 90 (2007) 132121.
[53] N. Tombros, C. Jozsa, M. Popinciuc, H.T. Jonkman, B.J. van Wees, Nature 448 (2007) 571.
[54] B.T. Jonker, G. Kioseoglou, A.T. Hanbicki, C.H. Li, P.E. Thompson, Nat. Phys. 3 (2007) 542.